High Field ^{33}S Solid State NMR and First-Principles Calculations in Potassium Sulfates

Igor Moudrakovski,* Stephen Lang, Serguei Patchkovskii, and John Ripmeester

Steacie Institute for Molecular Sciences, National Research Council, 100 Sussex Drive, Ottawa, K1A 0R6, Ontario, Canada

Received: August 25, 2009; Revised Manuscript Received: October 16, 2009

A set of potassium sulfates presenting a variety of sulfur environments (K_2SO_4, $KHSO_4$, $K_2S_2O_7$, and $K_2S_2O_8$) has been studied by ^{33}S solid state NMR at 21 T. Low natural abundance (0.75%) and small gyromagnetic ratio of ^{33}S presented a serious challenge even at such a high magnetic field. Nevertheless, using the QCPMG technique we were able to obtain good signals from the sites with C_Q values approaching 16 MHz. Assignment of the sites and the relative orientations of the EFG tensors were assisted by quantum mechanical calculations using the Gaussian 98 and CASTEP packages. The Gaussian 98 calculations were performed using the density functional method and gauge independent atomic orbitals on molecular clusters of about 100−120 atoms. The CASTEP calculations utilized periodic boundary conditions and a gauge-including projector augmented-wave pseudopotential approach. Although only semiquantitative agreement is observed between the experimental and calculated parameters, the calculations are a very useful aid in the interpretation of experimental data.

Introduction

Sulfates are very common and technologically a very important class of chemicals.[1] Their applications range from solid electrolytes in fuel cell applications[2] to construction[3] and agro-chemistry.[4] The properties of sulfates depend greatly on the local environment of sulfur, and ^{33}S solid state (SS) NMR could potentially play a significant role in studies of the chemistry of these materials. The technique, however, has seen very few applications, with just over 10 publications on the subject being produced in the past 25 years.[5−16] The problem arises mainly from the great difficulty in obtaining the spectra. The only magnetically active isotope, ^{33}S, has a low natural abundance of 0.75%, and is a spin 3/2 quadrupolar nucleus with rather small magnetogyric ratio γ (absolute resonance frequency Θ = 7.676 MHz). Low natural abundance and resonance frequency together with a moderate quadrupole moment of −8.17 fm^2 make ^{33}S SS NMR quite a challenging exercise. When the sulfur is not in a highly symmetric environment, such as the cubic site occupied in many sulfides,[5,7,8] the observed signals of central transitions are commonly broadened by the second-order quadrupolar interaction,[17,18] drastically reducing the intensity of the signals. An additional complication commonly encountered in SS NMR of low-γ nuclei is rather long relaxation times. In a case of ^{33}S, T_1 values as long as tens of seconds can be expected,[8,9] seriously hindering signal averaging. One should note that previously published ^{33}S SS NMR data deal mainly with situations of rather small quadrupolar interactions. Most reported quadrupolar coupling constants are in the range of 0−1.5 MHz, with the largest reported quadrupolar constant C_Q for a sulfate being just over 2 MHz, as reported for $BaSO_4$.[10] A question arises as to whether the reported quadrupolar constants truly represent the range of electric field gradients in sulfates. It is quite likely that these small C_Q values are simply due to limitations of available experimental techniques, which allowed only the study of a rather narrow range of environments. Indeed, a recent study of ^{33}S in layered sulfides of transition metals[16] demonstrated that significantly larger quadrupolar constants of up to 9.3 MHz that were accessible at the high magnetic field of 21.1 T.

In this work we studied a set of potassium sulfates with various sulfur environments, both for exploring the limits of ^{33}S SS NMR at the magnetic field of 21.1 T, and evaluating two different computational approaches of nuclear magnetic resonance parameters. The first method uses Gaussian 98[19] density functional theory (DFT) code and calculations are performed on relatively large specially constructed clusters. The second technique employs CASTEP, a recently developed ab initio quantum mechanical program.[20] The method is based on density functional theory and the plane-wave pseudopotential approach and is specifically designed for periodic systems such as crystals. Recently, the CASTEP calculations were successfully used in several SS NMR studies with some excellent results.[21−25]

Using a combination of high magnetic field of 21 T and the sensitivity enhancing quadrupolar Carr−Purcell−Meiboom−Gill (QCPMG) technique[26] we were able to obtain good quality ^{33}S SS NMR spectra of very broad signals. Our data demonstrate the magnitude of the ^{33}S quadrupole interactions in sulfates depends dramatically on the local symmetry of sulfur, with the quadrupole coupling constants ranging from a mere 1 MHz for potassium sulfate K_2SO_4 to over 16 MHz for the potassium pyrosulfate $K_2S_2O_7$. Both the range of the chemical shifts (CS) and the chemical shift anisotropy (CSA) in sulfates are relatively small, and the observed spectra are dominated by the second-order quadrupole interaction. The quadrupole coupling constants observed in this work are significantly larger than those reported in previous studies, and significantly extend the range of known C_Q values for sulfates. For all studied materials the results of the first-principles calculations are in good, and in some cases in excellent, agreement with the experimental data.

* Corresponding author: Phone: 613-993-5638, Fax: 613-990-1555, E-mail: igor.moudrakovski@nrc-cnrc.gc.ca.

10.1021/jp908206c
Published on Web 10/30/2009

Experimental Part

Materials. Potassium sulfate, K_2SO_4, potassium bisulfate, $KHSO_4$, and potassium persulfate, $K_2S_2O_8$, were commercial products (Aldrich, 99.5% grade) and were used without further treatment. The highly hygroscopic potassium pyrosulfate, $K_2S_2O_7$, was prepared by thermal decomposition of $K_2S_2O_8$ at 250 °C for 24 h[27] and was handled in a drybox in atmosphere of dry argon. The purity of materials was confirmed by powder XRD and ^{39}K MAS NMR.

NMR Measurements. The majority of ^{33}S NMR measurements were performed at 69.03 MHz on a Bruker Avance-II 900 MHz instrument (magnetic field of 21.14 T). The magic angle spinning (MAS) experiments were performed using Bruker single-channel 7 mm low-γ probe with dry nitrogen as a carrier gas. A simple single-pulse sequence was used to acquire the MAS spectra. The solution $\pi/2$ pulse was 10 μs, and the corresponding selective solid $\pi/2$ pulse was scaled by a factor of 2 to 5 μs.[17] Preacquisition delay prior to collection of the data was 10 μs. Static QCPMG[26] and spin−echo powder spectra were obtained on a home-built 7 mm solenoid probe. Pulses in the spin−echo sequence were optimized to reproduce the powder line shapes accurately.[28] The echo delays in QCPMG trains were set between 100 and 500 μs, and from 40 to 80 echoes were usually accumulated. In situations when the whole spectral range could not be excited in a single experiment (all compounds except K_2SO_4), the spectra were obtained from several equally spaced offsets. The distance between the offsets was selected to be a multiple of the separation between the spikelets in the QCPMG spectra, and the resulting subspectra were coadded. Several ^{33}S spectra of K_2SO_4 were also obtained at a lower field of 9.4 T on a Bruker DSX 400 MHz instrument (Larmor frequency 30.7 MHz). A home-built static probe and a 7 mm Bruker BL7 MAS probe were used in these measurements. A dual frequency sweep sensitivity enhancing technique[29] was used in some of the experiments at the lower field.

The ^{33}S signal from 2 M Cs_2SO_4 was used as an external secondary chemical shift reference and was set to 333 ppm relative to pure CS_2.[30] All spectra were recorded at room temperature.

The time domain data were processed with the NMR Tools[31] add-on package for the Origin graphing and analysis software,[32] allowing for a very flexible use of comb filters during processing of QCPMG data[33] and in general spectra manipulations. A Gaussian comb with the width of the components set at 25% of an echo window and centered at the maximum of echoes was employed. Analytical simulations of ^{33}S spectra were carried out using the WSolids SS NMR simulation package.[34]

Details of Computations. Plane-wave based DFT calculations of nuclear magnetic shielding and electric field gradient tensors were performed using the NMR module of the CASTEP DFT program, employing the gauge including projector augmented wave (GIPAW) algorithm.[20] CASTEP is part of Accelrys Materials Studio simulation and modeling package.[35] The Perdew Burke Ernzerhof (PBE) functional was used with the generalized gradient approximation (GGA) for all calculations.[36] The convergence of the calculated NMR parameters with the size of a Monkhorst−Pack k-point grid and a basis set cutoff energy were tested for all systems. The sufficient basis sets cutoff energies were 550 eV, and the k-point spacing was always smaller than 0.03 Å^{-1}. Unit cell parameters and atomic coordinates were taken from the most recent published structures for K_2SO_4,[37] $KHSO_4$,[38] $K_2S_2O_7$,[39] and $K_2S_2O_8$.[40] All CASTEP calculations were performed on a dual core Pentium 2.6 GHz computer with 4 GB of memory and average time for a single calculation ranging from 20 to 72 h.

Gaussian 98 (G98) calculations of the CSA and EFG tensors were carried out using the charge embedded cluster model.[41] The methods chosen and convergence properties were actually developed and tested during other work on ^{39}K NMR, and may not be fully optimized for ^{33}S. In view of the time-consuming nature of these tests and the similarity of the computational problem, the various tests were not repeated for ^{33}S. The B3YLP functional was used for all calculations reported here. Gaussian input files for charge-embedded clusters were created using software developed here, with only minor hand-tuning of an input file required for each system. The atom of interest is placed at the center of the cluster and is assigned the 6-311G(2d,2p) basis. Near neighbors, within about 4 Å, are assigned a 6-311G basis, and more distant atoms, as far away as 8.5 Å, are assigned the STO-3G basis. About 14 000 point charges were placed at lattice points to a radius of 40 Å around the cluster. Since calculating the EFG was the main goal, it was deemed essential to add and scale these charges to correctly reproduce the Madelung potential at the site of the atom of interest.[42] Calculations were carried out on a cluster, but were not parallelized. Each node is a DELL GX270 workstation with 2 GB of RAM, and calculation times varied from 24 to 48 h.

The calculations produce the absolute shielding tensors and the electric field gradients in the molecular frame. Diagonalization of the tensors provides the principal components (eigenvalues) and principal axis (eigenvectors). The calculated quadrupolar constants are found according to $C_Q = eQV_{zz}/h$, where Q is the quadrupolar moment of ^{33}S (−0.0678 barn[43]), and V_{zz} is the largest principal component of the electric field gradient (EFG) tensor. The asymmetry $\eta_Q = (V_{XX} - V_{YY})/V_{ZZ}$, with the EFG tensor components ordered as $|V_{ZZ}| \geq |V_{YY}| \geq |V_{XX}|$. The calculated quadrupolar parameters can be directly compared to the experimental data.

The calculated shielding parameters are described in Haeberlen convention[44,45] and include isotropic shielding $\sigma_i = 1/3\mathrm{Tr}\{\sigma\}$, the shielding anisotropy $\Delta\sigma = \sigma_{ZZ} - (\sigma_{XX} + \sigma_{YY})/2$, and asymmetry parameter $\eta_{CS} = (\sigma_{XX} - \sigma_{YY})/(\Delta\sigma - \sigma_{ZZ})$. The principal components of the symmetric shielding tensor ordered as $|\sigma_{ZZ} - \sigma_i| \geq |\sigma_{XX} - \sigma_i| \geq |\sigma_{YY} - \sigma_i|$. In order to compare the calculated absolute shielding constants and experimental chemical shifts measured relative to a reference material (CS_2 is commonly accepted as a reference compound in ^{33}S NMR), the calculated absolute shielding values need to be converted to the relative chemical shift scale. Ideally, one could do this by using the experimental ^{33}S absolute shielding scale.[46−48] The existing scale,[47,48] however, is for diluted gases and would require a correction for the effect of intermolecular interactions in CS_2. The effect is unknown, but may be as large as tens of ppm. To avoid the uncertainty we used secondary references. This can be done by performing additional calculations on reference molecules with known chemical shifts. All the shielding constants obtained in G98 calculations were referenced to the ^{33}S shielding constant in cubic magnesium sulfide MgS obtained at the same level of theory as in other calculations. The convergence of the isotropic shielding in MgS was tested in a series of clusters with radii ranging from $r = 5.8$ Å (33 atoms) to $r = 8.5$ Å (147 atoms). The isotropic chemical shifts are found then as $\delta_{iso}(\mathrm{ppm}) = \sigma_{MgS} - \sigma_i - 174.9$, where $\sigma_{MgS} = 663.3$ ppm (the value for cluster with $r = 8.2$ Å) and 174.9 is the chemical shift of MgS relative to CS_2.[8] Lower computational cost of CASTEP calculations allows for a higher accuracy in relating the absolute shielding to the chemical shift

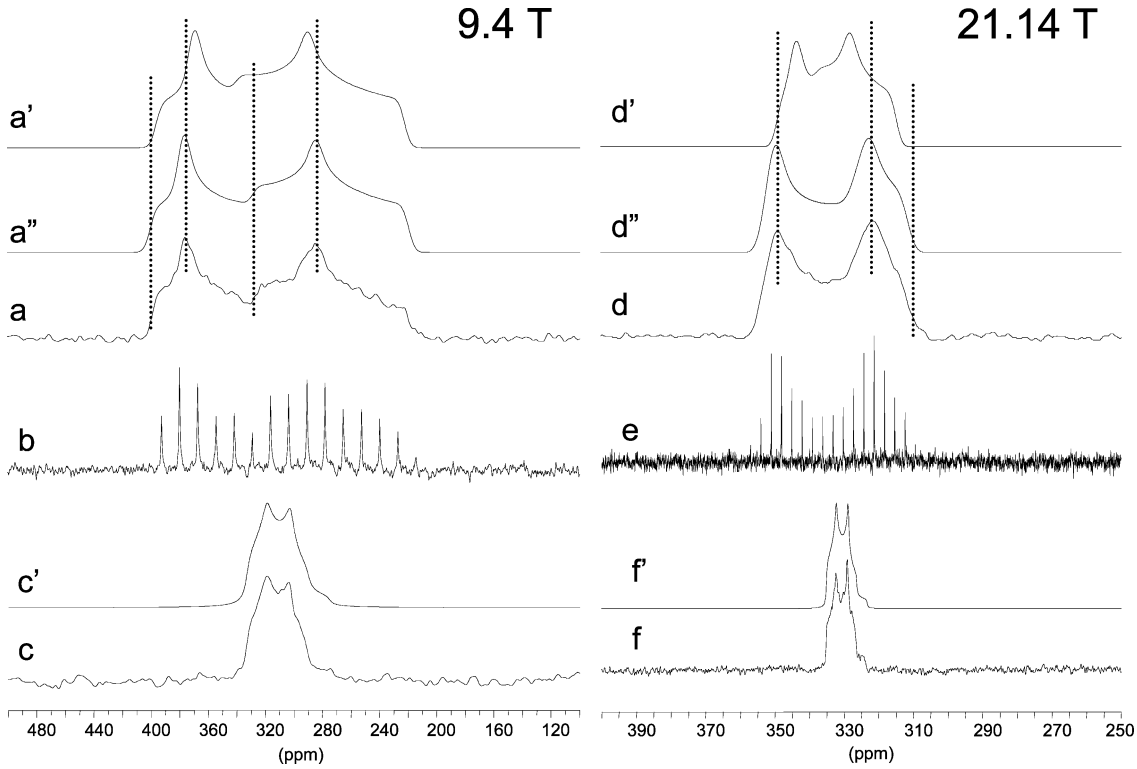

Figure 1. ^{33}S stationary Hahn-echo (a, d), QCPMG (b, e), and MAS (c,f) spectra of K_2SO_4 at 9.4 and 21.14 T. Traces a′, d′, c′, and f′ are the spectral fits to the experimental spectra accounting only for quadrupolar interactions. Traces a″ and d″ are the fits that also include the CSA.

by using a larger set of reference materials. The CASTEP isotropic shielding constants in 22 sulfates and sulfides obtained at the same level of theory were correlated to their experimental ^{33}S chemical shifts from refs 8−12. The correlation is illustrated in Figure S1 in the Supporting Information. The isotropic shift in this case is related to the shielding as $\delta_{iso}(ppm) = -0.977\sigma_i + 416.4$ ($R = 0.993$).

Results and Discussion

This section describes experimental and computational results for each compound studied, and discusses the relation of the solid state ^{33}S NMR parameters to the local sulfur environment in sulfates.

Potassium Sulfate, K_2SO_4. At ambient temperature the crystal structure of potassium sulfate is orthorhombic with space group *Pmcn* and 4 formula units per unit cell (low temperature form β-K_2SO_4).[37] There is one unique site for sulfur, two sites for potassium atoms, and three sites for oxygen. The crystal structure is built by packing of monomeric anions and potassium cations. There are two crystallographic mirror planes in the cell (at $x = 1/4$ and $x = 3/4$), and all the atoms lie in these planes except two oxygen atoms (O(3) and (O(3′)) of each formula unit, which lie approximately midway between the mirror planes. The sulfate anions have crystallographicaly imposed ***m*** symmetry. The interatomic distances SO(1), SO(2), SO(3) and the four bond angles within the anions are 1.475, 1.485, 1.484 Å, and 110.55°, 109.67°, 108.79°, and 109.35° .[37] Usually, the first coordination sphere plays the most significant effect on the NMR parameters, and the site symmetry may impose constrains on the orientation of the CSA and EFG tensors. In a case of K_2SO_4, the presence of sulfur on a mirror plane requires that one component of each tensor be perpendicular to the plane, and the others must be in the plane. The very small differences between the lengths of the S−O bonds, however, suggest a relatively small EFG on the sulfur atom. Since all four O−S−O angles are different, we may also expect a noticeable deviation of the quadrupolar asymmetry parameter η_Q from 0.

Eckert and Yesinowski[5] estimated the upper limit for the quadrupolar coupling constant C_Q in K_2SO_4 at 1.13 MHz with no asymmetry parameter η_Q reported. The more recent study[9] gives $C_Q = 0.97$ MHz and $\eta_Q = 0.50$. The ^{33}S isotropic shift in K_2SO_4 was reported at 334 ± 3 ppm[5] and 336 ppm.[9] Considering that the first value was obtained from a stationary spectrum,[5] and the second value has been obtained from MAS spectrum at a substantially higher magnetic field,[9] the later is likely to be more accurate. The results of a recent study[14] confirm the data of ref 9. A peak position in ^{33}S MAS spectrum for K_2SO_4 has been also reported in ref 10, but it does not state if a correction for the second order quadrupolar shift has been made.

The experimental ^{33}S NMR spectra of potassium sulfate at 9.4 and 21.1 T, along with the analytical simulations using a model for central transition of spin 3/2 affected by the second-order quadrupolar interactions, with and without contribution of the CSA, are shown in Figure 1. The estimated relaxation time T_1 in this compound is 15 s, and even with the use of DFS it took over 34 h to obtain a decent spin−echo spectrum at 9.4 T. Acquiring the signal with a QCPMG pulse sequence resulted in a significant reduction of time, nevertheless it still takes over 12 h to acquire a usable signal. The isotropic chemical shift δ_{iso}, quadrupolar coupling constant C_Q, and asymmetry parameter η_Q obtained from the fits of experimental MAS spectra are listed in Table 1 and agree well with the previously reported values. Close inspection of the stationary spectra obtained at different fields reveals that their lineshapes cannot be fully accounted for by only second-order quadrupolar interactions, and the chemical shift anisotropy has also to be taken into account. It becomes particularly obvious if one tries to fit the stationary spectra using the δ_{iso}, C_Q, and η_Q obtained from the MAS spectra. A combined fit with both the EFG and CSA interactions reveals the chemical shift anisotropy $\Delta\delta$ of −17.5

TABLE 1: Experimental and Calculated ^{33}S SS NMR Parameters in Potassium Sulfates

	experimental data					calculated data						
compound	δ_{iso}, ppm	$\Delta\delta$, ppm	η_{CSA}	C_Q, MHz	η_Q	σ_i, ppm	δ, ppm	$\Delta\delta$,[e] ppm	η_{CSA}	C_Q, MHz	η_Q	calculation method
K_2SO_4	335.7[a]	−17.5 ± 4[b]	0.3[b]	0.959[a]	0.42[a]	103.9	314.9	−20.9	0.27	0.924	0.35	CASTEP
						138.1	350.3	8.3	0.89	0.405	0.44	G98
$KHSO_4$ S−I	330[c,d]			10.6[c]	0.38[c]	118.60	300.5	178.1	0.93	10.95	0.30	CASTEP
S−II						122.00	297.2	175.1	0.38	10.77	0.53	CASTEP
S−I						154.1	334.3	203.8	0.69	12.74	0.16	G98
S−II						152.9	335.5	202.8	0.27	12.6	0.24	G98
$K_2S_2O_7$	320[c,d]			16.2[c]	0.1[c]	141.8	293.1	208.2	0.09	15.16	0.39	CASTEP
						154.1	334.3	205.2	0.09	15.72	0.27	G98
$K_2S_2O_8$	330[c,d]			15.9[c]	0.1[c]	139.1	280.5	190.8	0.11	14.96	0.07	CASTEP
						155.9	332.5	188.0	0.06	15.64	0.05	G98

[a] The reported experimental parameters are from the best fit of 21.1T MAS spectrum; estimated error is 0.3 ppm. [b] The reported experimental parameters are from the best fit of 21.1T stationary spectrum constrained by the EFG parameters and δ_{iso} from the 21.1T MAS spectrum. [c] The reported experimental parameters are from analytical simulation of the observed signal considering only quadrupolar interactions. [d] The error in ^{33}S δ_{iso} for $KHSO_4$, $K_2S_2O_7$, and $K_2S_2O_8$ is estimated to be less than ±50 ppm. [e] Haeberlen convention for the chemical shift tensor is used.[44,45] Note that the calculated anisotropy is reported in the chemical shift scale where it has the sign opposite to that in the shielding scale.

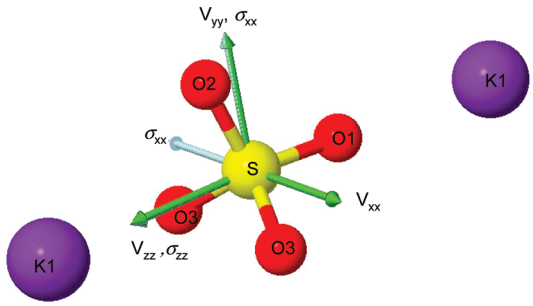

Figure 2. Orientation of EFG (V_{XX}, V_{YY}, V_{ZZ}) and chemical shielding (σ_{XX}, σ_{YY}, σ_{ZZ}) tensors of sulfur in relation to SO_4 group of potassium sulfate.

ppm and the asymmetry parameter η_{CS} of 0.3. The experimental Euler angles provide the orientation of the chemical shielding tensor in relation to the EFG tensor. The only nonzero angle is γ at 90°. In this arrangement the z-axes of both tensors coincide, when the other two pairs of axes remain in the same plane rotated counterclockwise by 90°. No ^{33}S chemical shift anisotropy in K_2SO_4 has been reported previously, and this is a first report of a ^{33}S CSA in sulfates. Most likely, the anisotropy was not detected previously because the spectra in ref 5 were obtained only for a stationary sample at one magnetic field with significantly lower signal-to-noise ratio. In a later study,[9] on another hand, no measurements of stationary samples were made, and the anisotropy was averaged by the MAS.

The experimental data together with the results of DFT calculations for the embedded cluster approximation and periodic boundaries condition method are summarized in Table 1. For both computational methods the calculated isotropic chemical shift is only in fair agreement with the experimental data. In a case of G98, the δ_{iso}^{Calc} is overestimated by about 15 ppm, whereas for CASTEP the value is underestimated by about the same margin. The orientations of the CS and EFG tensors in molecular frame are shown in Figure 2. A close look at the crystal structure reveals that the most shielded component of the CS tensor and the largest component of the EFG tensor both lie on the same line passing through K1−O1−S1−K1 atoms in the {0.25,0,0} plane and oriented in the same directions, in complete agreement with the experimental data and the site symmetry. One should note, however, that the reported set of Euler angles is not unique and there are other sets of Euler angles[45] defining the same relative orientation of the CS and EFG tensors.

The C_Q from the G98 calculation is noticeably smaller than observed experimentally or found from the calculations using periodic boundary conditions. A discrepancy between calculated and experimental C_Q of sulfur in potassium sulfate has been observed previously[9] and was attributed to the limited size of the cluster used in calculations. As we will see later from the results for other salts, the truncation effects of the lattice can not explain the poor agreement for K_2SO_4.

Potassium Bisulfate, $KHSO_4$. The hydrogen sulfates $MHSO_4$ (M = NH_4, Na, K, Rb, Cs) form an interesting group of materials characterized by the presence of a hydrogen bonding pattern between the HSO_4^- ions. The structure of $KHSO_4$ is orthorhombic. The space group is *Pbca*, a = 8.429 Å, b = 9.807 Å, c = 18.976 Å, and there are two HSO_4^- ions in the asymmetric unit.[38] One of the two ions is linked to a polymeric chain by hydrogen bonding along a glide plane, the other forms a dimer across the center of symmetry.[38] Thermoelastic properties and phase transitions in $KHSO_4$, and their relation to the hydrogen bonding were extensively studied.[49−51] The interatomic distances in the two HSO_4 groups are S1−O2: 1.467 Å, S1−O1: 1.574 Å, S1−O3: 1.441 Å, S1−O4 1.443 Å, O1−H1: 0.746 Å; S2−O5: 1.475 Å; S2−O6: 1.565 Å, S2−O7: 1.444 Å, S2−O8: 1.438 Å, O6−H2 0.805 Å. The longest S−O bonds are those connected to the protons, and considering that these bonds are significantly longer than three others (over 0.1 Å in the first, and 0.09 Å for the second site), one may expect larger EFGs at both sulfur sites.

The ^{33}S QCPMG spectrum of $KHSO_4$, acquired in eight frequency offsets, is shown on Figure 3. The spectrum is visibly dominated by the second-order quadrupolar interaction. Since the total span of the frequencies in the stationary spectrum is close to 250 kHz, any attempt of using MAS with currently available spinning speed of generally less than 50 kHz would be unproductive. Although some narrowing of the signal could be achieved, the resulting spectrum would unlikely be of any value due to the overlapped spinning sidebands and distortion of the central signals because of insufficient spinning speed. The limited spectral resolution certainly hampers the analysis, but some valuable information can still be extracted. The observed spectrum can be reasonably well simulated with just one signal, as it shown on Figure 3. In this case the absence of significant signs of multiple signals is a strong indication of

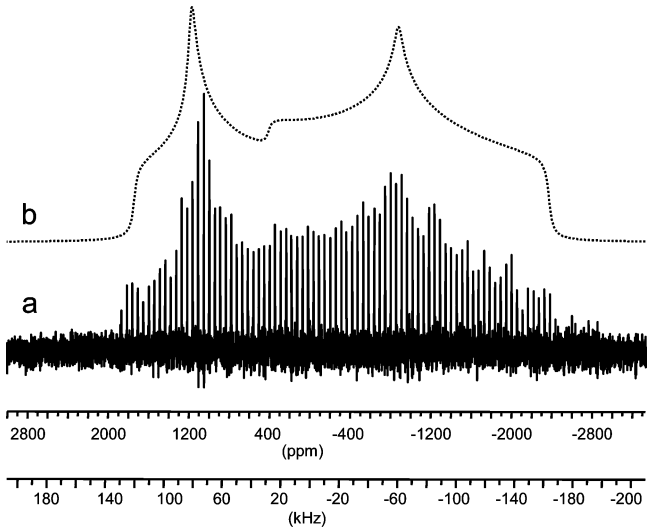

Figure 3. ^{33}S QCPMG spectrum of $KHSO_4$ at 21.14 T (a). The spectrum has been obtained by coadding of eight equally offset subspectra. Each subspectrum is a result of 4000 accumulations with 8 s delay. The upper trace (b) is WSolids simulation of the spectrum using a single site and a model for the central transition of spin 3/2 with quadrupolar parameters shown in Table 1.

rather close spectral parameters for the two signals of equal intensity. The fit results in $C_Q = 10.6$ MHz, $\eta_Q = 0.38$, $\delta_{iso} = 330$ ppm. As we have already mentioned, previous studies of solid state ^{33}S NMR were limited to systems with rather small quadrupolar constants. The observed C_Q of over 10 MHz demonstrates both the sensitivity of the method to the variation of the structure, and a drastic improvement in signal detection resulting from the use of the highest available magnetic fields.

The results of DFT calculations for both the cluster approximation and periodic boundary conditions are summarized in Table 1. Due to the excessive broadening of the experimental spectrum by strong quadrupolar interactions that can not be even partially reduced by currently available techniques, the calculated and experimental shielding parameters can be compared only qualitatively. The experimental isotropic shift of $KHSO_4$ appears to be in the same range as for K_2SO_4, or about 330 ppm, and within experimental error is consistent with the values obtained by the two calculation approaches. Both the Gaussian and CASTEP results suggest only a minor difference (2−4 ppm) in the isotropic shielding constants for the two inequivalent sulfur sites, and that both sites are 10−15 ppm more shielded than the sulfur site in K_2SO_4. The calculations predict nearly equal and substantial anisotropies of the shielding for both sites. The values produced by the Gaussian calculations are slightly larger at about 200 ppm, compared to approximately 175 ppm from CASTEP. Our attempts to verify that the anisotropy does indeed influence the experimental data were unsuccessful. This was due mostly to the limited resolution of the QCPMG data and a comparatively small contribution of anisotropy to the experimental line shape. The complete analysis of all interactions is obviously not possible at this time: there are two sites with eight variables for each site, and only a relatively low resolution spectrum obtained at a single field. The quadrupolar parameters obtained by both computational methods are in very good accord with the experimental data. The agreement of the CASTEP data is particularly good, where the quadrupolar constant is overestimated by only 5% and the asymmetry parameters are well in the range of observed in the experiment. Even though the C_Q values from the Gaussian calculations at 12.6 and 12.74 MHz are about 20% higher than the experimentally observed value,

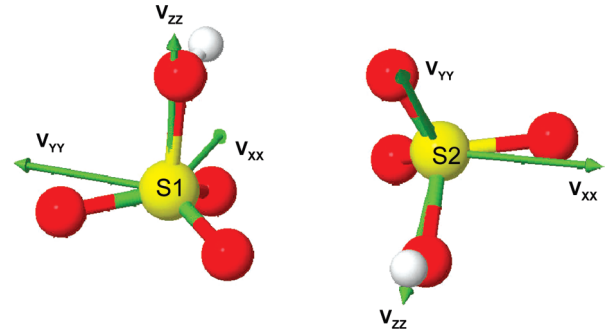

Figure 4. Calculated orientations of the EFG tensors for two sulfur sites in the crystal of $KHSO_4$ (CASTEP data). The total crystal structure is a superposition of the two H SO_4 units shown.

and the asymmetry parameters are somewhat underestimated, the obtained numbers are still very reasonable, considering the ionic character of the material. Although the inclusion of the periodicity of the lattice in the calculation is likely a factor contributing to a better agreement of the EFG parameters from CASTEP, the benefit of this approach in this particular case is not that obvious.

The calculated orientations of the EFG tensors for the both sulfur sites in the molecular frame are shown in Figure 4. For both sites the largest principal component of the EFG tensor, V_{ZZ}, lies along the sulfur−oxygen bond of the S−O−H group. In this situation the hydrogen bonds within the crystal define the gradients of electric field.

Potassium Pyrosulfate, $K_2S_2O_7$. Potassium pyrosulfate represents an example of condensed sulfate groups. The compound crystallizes in monoclinic space group $C2/c$, $a = 12.35$ Å, $b = 7.31$ Å, $c = 7.27$ Å, $\beta = 93.12°$, with 4 formula units per unit cell.[39] There is a unique site for sulfur, one site for potassium, and four nonequivalent sites for oxygen. The pyrosulfate ion is bent with the bridging angle of 124.2°, and the bridging oxygen atom (O(4)) lies on a 2-fold axis relating the two SO_3 groups in each anion. The interatomic distances within SO_3 groups SO(1), SO(2), SO(3), S(4) are 1.438, 1.428, 1.447, 1.645 Å, and the angles O(1)−S−(O4), O(2)−S−O(4), O(3)−S−O(4), O(1)−S−O(2), O(1)−S−O(3), and O(2)−S−O(3) are 106.1°, 101.3°, 106.2°, 115.5°, 112.8°, and 113.6°.[39] Considering that the bridging S−O(4) bond is substantially longer that the three remaining bonds S−O, one may expect a substantial EFG on the sulfur atom. Although the SO_3 groups do not have axial symmetry, such a small variation in the lengths of S−O bonds and the O−S−O angles suggests only small deviation of the quadrupolar asymmetry parameter from zero.

The experimental ^{33}S QCPMG spectrum of $K_2S_2O_7$ spans over 600 kHz and has been acquired using 14 frequency offsets (Figure 5). The singularities in the spectrum are well-defined, and the total envelope can be simulated with a model of the central transition affected by the second-order quadrupolar using the following parameters: $\delta_{iso} = 320 \pm 50$ ppm, $C_Q = 16.2 \pm 0.15$ MHz, and $\eta_Q = 0.1 \pm 0.05$. Due to the very large frequency span of the spectrum, the error in obtaining the isotropic chemical shift is relatively large. It appears that at this stage it would be too speculative to discuss whether the powder spectrum of $K_2S_2O_7$ shows distinct signs of contribution from the chemical shift anisotropy. The experimental spectrum, however, does deviate from an ideal quadrupole only line shape, pointing into some unaccounted contributions.

The results of G98 and CASTEP calculations together with the experimental data are summarized in Table 1. Both calculations correctly predict that the experimental isotropic shift

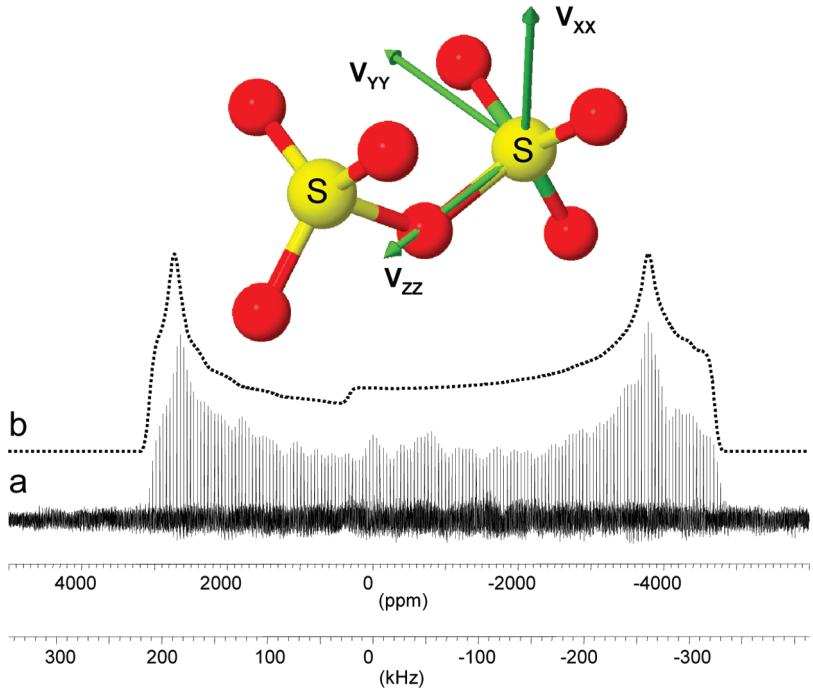

Figure 5. ^{33}S QCPMG spectrum of $K_2S_2O_7$ at 21.14 T (a). The spectrum has been obtained by coadding of 14 equally offset subspectra. Each subspectrum is a result of 2000 accumulations with 10 s delay. The upper trace (b) is WSolids simulation of the spectrum using a single site and a model of the central transition of spin 3/2 with quadrupolar parameters shown in Table 1. The inset demonstrates the calculated orientation of the EFG tensor (CASTEP data).

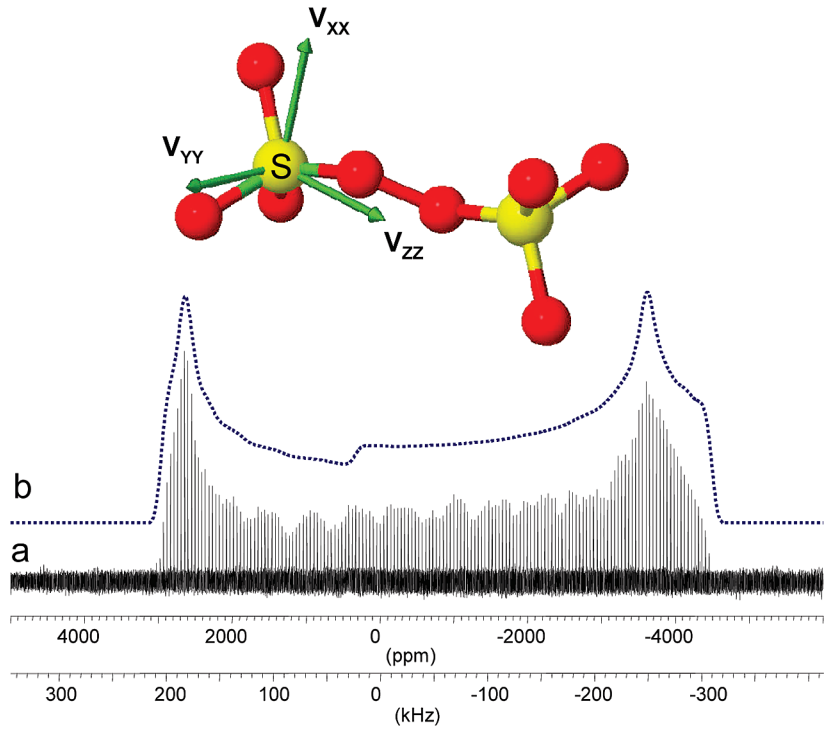

Figure 6. ^{33}S QCPMG spectrum of $K_2S_2O_8$ at 21.14 T (a). The spectrum has been obtained by coadding of 14 equally offset subspectra. Each subspectrum is a result of 2000 accumulations with 10 s delay. The upper trace (b) is WSolids simulation of the spectrum using a single site and a model for the central transition of spin 3/2 with quadrupolar parameters shown in Table 1. The inset shows the calculated orientation of the EFG tensor (CASTEP data).

of $K_2S_2O_7$ is similar to K_2SO_4 and $KHSO_4$, or about 320−340 ppm. Both the Gaussian and CASTEP data suggest approximately 200 ppm anisotropies, but as noted above this cannot be experimentally verified. A potentially accurate determination of the chemical shift anisotropy is possible through single crystal studies. This, however, would require either a very large single crystal, or preparation of a highly ^{33}S enriched single crystal. Neither approach is promising enough to pursue at this time. The quadrupolar parameters from both computational approached are in very good agreement with experiment, although a little underestimated. The C_Q from G98 in this case is closer to that observed, differing by only 3%. The asymmetry

parameters, however, from both computational methods are greater than observed, but still in the reasonable agreement. Again, G98 result is closer to experiment.

Potassium Persulfate, $K_2S_2O_8$. In potassium persulfate the two sulfate groups are connected by a covalent bond between oxygen atoms, potentially changing the EFG at the ^{33}S site. The crystal is triclinic, space group $P1$, with $a = 5.115$, $b = 7.034$, $c = 5.505$ Å, $\alpha = 106.32$, $\beta = 90.18$, $\gamma = 106.12°$, and one molecule per unit cell.[40] The structure contains unique sites for potassium and sulfur and four different sites for oxygen. The $S_2O_8^{2-}$ persulfate anion in a crystal possesses point symmetry C_i with the center of inversion located between the interconnected O(1) atoms. The interatomic distances in the persulfate anion S−O(1), S−O(2), S−O(3), and S−O(4) are 1.645, 1.421, 1.425, and 1.429 Å, and the angles O(1)−S−(O2), O(2)−S−O(3), O(2)−S−O(4), and O(3)−S−O(4) are 98.2°, 115.5°, 116.6°, and 113.2°.[40] Similar to the pyrosulfate anion, one S−O distance in each sulfate group of the persulfate anion is significantly longer than the three others, which is expected to result in a large electric field gradient on sulfur atom, and a large C_Q. The local symmetry on the sulfur is again close to C_3 suggesting rather small quadrupolar asymmetry parameter η_Q.

The very large experimental C_Q value of 15.9 MHz and $\eta_Q = 0.1$ (the spectrum is shown in Figure 6) are in good agreement with these qualitative expectations. The experimental results are confirmed by the first principles calculations. The EFG parameters from the G98 and CASTEP calculations are well within the experimental error of the experiments and perhaps in the best agreement among all studied compounds. Similar to $KHSO_4$ and $K_2S_2O_7$, the experimental error in the experimental chemical shift is too large for a detailed discussion of the ^{33}S shielding. All indications are that the isotropic shift in $K_2S_2O_8$ is likely not too far from that in K_2SO_4, that is, around 330 ppm. This compares well with the isotropic chemical shift of 319 ppm recently reported for $K_2S_2O_8$ in saturated water solution.[52] Apparently the effects of solvent and the crystal lattice have relatively small effect on the isotropic chemical shift of the sulfate group. In accord, the calculations predict only small differences in the isotropic shifts of the sulfate groups, which are in the quite different environments for all four compounds studied. The calculated shielding anisotropy has the same sign and is very close in magnitude to that in $K_2S_2O_7$, which is not too surprising given the similarity in the geometry of the SO_4 groups in these two compounds.

Conclusions

We report results of a natural abundance ^{33}S SS NMR study in four potassium sulfates. Use of a high field 21 T magnet, in combination with acquiring the spectra using the QCPMG technique, resulted in a great improvement of sensitivity, allowing detection of the spectra from the sites with reduced symmetry and very large quadrupolar constants, up to 16 MHz. For the first time, a chemical shift anisotropy has been reported for the sulfate ion, in K_2SO_4. The isotropic chemical shift appears to be relatively insensitive to the environment, whereas the quadrupolar parameters show great sensitivity even to relatively small variations in the S−O lengths and the symmetry of the SO_4 anions. The assignment of the sites and the relative orientations of the EFG tensors were assisted by first-principal calculations using Gaussian 98 and CASTEP packages. Both methods produce calculated magnetic resonance parameters in good agreement with experiment, demonstrating the great potential of modern computational techniques in SS NMR.

Acknowledgment. The authors thank Dr. Victor Terskikh for technical assistance. Access to the 900 MHz NMR spectrometer and Accelrys Materials Studio modeling package was provided by the National Ultrahigh Field NMR Facility for Solids (Ottawa, Canada), a national research facility funded by the Canada Foundation for Innovation, the Ontario Innovation Trust, Recherche Québec, the National Research Council Canada, and Bruker BioSpin and managed by the University of Ottawa (http://www.nmr900.ca).

Supporting Information Available: Correlation between the experimental chemical shifts and calculated absolute shieldings, table of calculated Euler angles, source code of the program used for generation of clusters for G98 calculations, complete G98 input files for all the clusters used in calculations. This information is available free of charge via the Internet at http://pubs.acs.org.

References and Notes

(1) Schmidt, M.; Siebert, W. *The Chemistry of Sulfur*; Pergamon Press: Oxford, England: 1975.

(2) *Industrial Applications of Batteries: From Cars to Aerospace and Energy Storage*; Broussely, M., Pistoia, G. Eds.; Elsevier: Oxford, U.K., 2007.

(3) *Concrete Technology: New Trends, Industrial Applications*; Proceedings of the International RILEM workshop; Barcelona, 1994; Aguado, A., Gettu, R., Shah, S. P. Eds.; Barcelona, 1994.

(4) *Natural Products in the New Millennium: Prospects and Industrial Application*; Proceedings of the Phytochemical Society of Europe; Rauter, A. P., Palma, F. B., Justino, J., Araújo, M. E. Eds.; Kluwer Academic Publishers: The Netherlands: 2002.

(5) Eckert, H.; Yesinowski, J. P. *J. Am. Chem. Soc.* **1986**, *108*, 2140.

(6) Bastow, T. J.; Stuart, S. N. *Phys. Status Solidi B* **1988**, *145*, 719.

(7) Daunch, W. A.; Rinaldi, P. L. *J. Magn. Res. A* **1996**, *123*, 219.

(8) Wagler, T. A.; Daunch, W. A.; Rinaldi, P. L.; Palmer, A. R. *J. Magn. Reson.* **2003**, *161*, 191.

(9) Wagler, T. A.; Daunch, W. A.; Panzner, M.; Youngs, W. J.; Rinaldi, P. L. *J. Magn. Reson.* **2004**, *170*, 336.

(10) Couch, S.; Howes, A. P.; Kohn, S. C.; Smith, M. E. *Solid State Nucl. Magn. Reson.* **2004**, *26*, 203.

(11) Jakobsen, H.; Hove, A. R.; Bildsoe, H.; Skibsted, J. *J. Magn. Reson.* **2006**, *180*, 170.

(12) d'Espinose de Lacaillerie, J.-B.; Barberon, F.; Bresson, B.; Fonollosa, P.; Zanni, H.; Fedorov, V. E.; Naumov, N. G.; Gan, Z. *Cem. Concr. Res.* **2006**, *36*, 1781.

(13) Jakobsen, H. J.; Hove, A. R.; Bildsøe, H.,; Skibsted, J.; Brorson, M. *Chem. Comm.* **2007**, 1629.

(14) Hansen, M. R.; Brorson, M.; Bildsøe, H.; Skibsted, J.; Jakobsen, H. *J. Magn. Reson.* **2008**, *190*, 316.

(15) O'Dell, L. A.; Klimm, K.; Freitas, J. C. C.; Kohn, S. C.; Smith, M. E. *Appl. Magn. Reson.* **2008**, *35*, 247.

(16) Sutrisno, A.; Terskikh, V. V.; Huang, Y. *Chem. Comm.* **2009**, 186.

(17) Freude, D.; Haase, J. Quadrupole effects in solid-state nuclear magnetic resonance. In *NMR Basic Principles and Progress*; Diehl, P.; Fluck, E.; Günther, H.; Kasfeld, R.; Seelig, J., Eds.; Springuel-Verlag: Berlin, 1993, pp 1−90; Vol *29*.

(18) Ashbrook, S. E.; Duer, M. J. *Concepts Magn. Reson. A* **2006**, *28*, 183.

(19) Frisch, M. J.; Trucks, G. W.; Schlegel, H. B.; Scuseria, G. E.; Robb, M. A.; Cheeseman, J. R. ; Montgomery J. A., Jr.; Vreven, T.; Kudin, K. N.; Burant, J. C.; Millam, J. M.; Iyengar, S. S.; Tomasi, J.; Barone, V.; Mennucci, B.; Cossi, M.; Scalmani, G.; Rega, N.; Petersson, G. A.; Nakatsuji, H.; Hada, M.; Ehara, M.; Toyota, K.; Fukuda, R.; Hasegawa, J.; Ishida, M.; Nakajima, T.; Honda, Y.; Kitao, O.; Nakai, H.; Klene, M.; Li, X.; Knox, J. E.; Hratchian, H. P.; Cross, J. B.; Bakken, V.; Adamo, C.; Jaramillo, J.; Gomperts, R.; Stratmann, R. E.; Yazyev, O.; Austin, A. J.; Cammi, R.; Pomelli, C.; Ochterski, J. W.; Ayala, P. Y.; Morokuma, K.; Voth, G. A.; Salvador, P.; Dannenberg, J. J.; Zakrzewski, V. G.; Dapprich, S.; Daniels, A. D.; Strain, M. C.; Farkas, O.; Malick, D. K.; Rabuck, A. D.; Raghavachari, K.; Foresman, J. B.; Ortiz, J. V.; Cui, Q.; Baboul, A. G.; Clifford, S.; Cioslowski, J.; Stefanov, B. B.; Liu, G.; Liashenko, A.; Piskorz, P.; Komaromi, I.; Martin, R. L.; Fox, D. J.; Keith, T.; Al.Laham, M. A.; Peng, C. Y.; Nanayakkara, A.; Challacombe, M.; Gill, P. M. W.; Johnson, B.; Chen, W.; Wong, M. W.; Gonzalez, C.; Pople, J. A. *Gaussian 98 (Revision A.11.3)*; Gaussian, Inc., Pittsburgh PA, 2002.

(20) Clark, S. J.; Segall, M. D.; Pickard, C. J.; Hasnip, P. J.; Probert, M. J.; Refson, K.; Payne, M. C. *Z. Kristallogr.* **2005**, *220*, 567.

(21) Ashbrook, S. E.; Berry, A. J.; Frost, D. J.; Gregorovic, A.; Pickard, C. J.; Readman, J. E.; Wimperis, S. *J. Am. Chem. Soc.* **2007**, *129*, 13213.
(22) Charpentier, T.; Ispas, S.; Profeta, M.; Mauri, F.; Pickard, C. J. *J. Phys. Chem. B* **2004**, *108*, 4147.
(23) Chappell, H.; Duer, M.; Groom, N.; Pickard, C.; Bristow, P. *Phys. Chem. Chem. Phys.* **2008**, *10*, 600.
(24) Ashbrook, S. E.; Le Polle, L.; Pickard, C. J.; Berry, A. J.; Wimperis, S.; Farnan, I. *Phys. Chem. Chem. Phys.* **2007**, *9*, 1587.
(25) Bryce, D. L.; Bultz, E. B.; Aebi, D. *J. Am. Chem. Soc.* **2008**, *130*, 9282.
(26) Larsen, F. H.; Jakobsen, H. J.; Ellis, P. D.; Nielsen, N. C. *J. Phys. Chem. A* **1997**, *101*, 8597.
(27) Mineely, P. J.; Tariq, S. A. *Aust. J. Chem.* **1984**, *37*, 191.
(28) Bodart, P. R.; Amoureux, J. P.; Dumazy, Y.; Lefort, R. *Mol. Phys.* **2000**, *98*, 1545.
(29) Kentgens, A. P. M.; Verhagen, R. *Chem. Phys. Lett.* **1999**, *300*, 435.
(30) Belton, P. S.; Cox, I. J.; Harris, R. K. *J. Chem. Soc. Faraday Trans. 2* **1985**, *81*, 63.
(31) Buess, M. NMR Tools for Origin, www.nmrtools.com.
(32) OriginPro 7.0; OriginLab; www.originlab.com.
(33) Lefort, R.; Wiench, J. W.; Pruski, M.; Amoureux, J.-P. *J. Chem. Phys.* **2002**, *116*, 2493.
(34) Eichele, K., Wasylishen, R. E. *WSolids NMR Simulation Package*, v. 1.17.26; 2000.
(35) *Accelrys Materials Studio*; v 4.1; www.accelrys.com.
(36) (a) Perdew, J. P.; Burke, K.; Ernzerhof, M. *Phys. Rev. Lett.* **1996**, *77*, 3865. (b) Perdew, J. P.; Burke, K.; Ernzerhof, M. *Phys. Rev. Lett.* **1997**, *78*, 1396.
(37) Ojima, K.; Nishihata, Y.; Sawada, A. *Acta Cryst. B* **1995**, *51*, 287.
(38) (a) Payan, F.; Haser, R. *Acta Cryst. B* **1976**, *32*, 1875. (b) Cotton, F. A.; Frenz, B. A.; Hunter, D. L. *Acta Cryst. B* **1975**, *31*, 302.
(39) Ståhl, K.; Balic-Zunic, T.; da Silva, F.; Eriksen, K. M.; Berg, R. W.; Fehrmann, R. *J. Solid State Chem.* **2005**, *178*, 1697.
(40) Naumov, D.Yu.; Virovetc, A. V.; Podberezskaya, H. B.; Novikov, P. B.; Politov, A. A. *Zhurn. Struct. Khim.* **1997**, *38*, 922.
(41) Stevens, F.; Van Speybroeck, V.; Pauwels, E.; Vrielinck, H.; Callens, F.; Waroquier, M. *Phys. Chem. Chem. Phys.* **2005**, *7*, 240.
(42) Sousa, C.; Casanovas, J.; Rubio, J.; Illas, F. *J. Comput. Chem.* **1993**, *14*, 680.
(43) Sundholm, D.; Olsen, J. *Phys. Rev. A* **1990**, *42*, 1160.
(44) Haeberlen, U. In *Advances in Magnetic Resonance*; Waugh, J. S., Ed.; Academic Press, New York: 1976; Suppl. 1.
(45) Mehring, M. *Principles of High Resolution NMR in Solids*, 2nd ed.; Springer-Verlag: Berlin, 1983.
(46) Wasylishen, R. E.; Mooibroek, S.; Macdonald, J. B. *J. Chem. Phys.* **1984**, *81*, 1057.
(47) Jackowski, K.; Makulski, W.; Kozminski, W. *Magn. Reson. Chem.* **2002**, *40*, 563.
(48) Makulski, W.; Jackowski, K. *J. Mol. Struct.* **2004**, *704*, 219.
(49) Cotton, F. A.; Diosa, J. E.; Vargas, R. A.; Mina, E.; Torijano, E.; Mellander, B.-E. *Phys. Stat. Sol. B* **2000**, *220*, 641.
(50) Abdel-Kader, M. M.; El-Shawarby, A.; Housny, W. M.; El-Tanahy, Z. H.; El-Kabbany, F. *Mater. Res. Bull.* **1994**, *29*, 317.
(51) Gerlich, D.; Siegert, H. *Acta Cryst.A* **1975**, *31*, 207.
(52) Aitken, R. A.; Arumugam, S.; Mesher, S. T. E.; Riddell, F. G. *J. Chem. Soc., Perkin Trans. 2* **2002**, 225.

JP908206C